Wettability Effect of the Surface Morphologies of *Musa acuminata* Leaves

Hasrawati Abu Hassan,[a] Mariyam Jameelah Ghazali,[a] Cevdet Meric,[b] and Che Husna Azhari [c]

The biomimetic application was studied for banana leaves (*Musa acuminata* Colla), which have been commonly used as a traditional cleaning technique for ironing plates. In this study, banana leaf surfaces were subjected to horizontal sliding forces of 5 N, 10 N, 15 N, and 30 N, using a heated plate at 100 °C, 200 °C, 300 °C, and 500 °C. The self-cleaning behavior of the banana leaves was determined by measuring the adhesion force, roughness, and contact angle, which were subsequently correlated with the surface morphology. Based on the results of this study, the adhesion force decreased from 6.39 nN ± 0.42 nN at 100 °C to 0.50 nN ± 0.50 nN at 500 °C with a load of 30 N, whereas the roughness increased from 0.79 µm ± 0.21 µm at 100 °C to 1.12 µm ± 0.30 µm at 500 °C. Furthermore, the contact angle decreased from 124.8° at 100 °C to 104.0° at 500 °C with a load of 30 N. This study established that the morphology of the banana leaves was altered with the temperature during sliding, which correlated with the surface characteristics.

Keywords: Banana leaves; Sliding test; Self-cleaning; Adhesion force; Roughness; Wettability

Contact information: a: Department of Mechanical and Materials Engineering, Faculty of Engineering and Built Environment, Universiti Kebangsaan Malaysia, 43600 UKM Bangi, Selangor, Malaysia; b: Faculty of Engineering, Fatih University, 34500 Buyukcekmece/Istanbul/Turkey; c: Kolej Permata INSAN, Universiti Sains Islam Malaysia, 71800 Nilai, N.Sembilan;
**Corresponding author: mariyam@eng.ukm.my*

INTRODUCTION

To develop more innovative technical applications, researchers have long been inspired by the natural environment to study the basic principles of structures, materials, and surfaces (Ghazali *et al.* 2016). The increasing demand for superhydrophobicity has also prompted investigations into potential biomimetic applications, such as self-cleaning, anti-corrosion, and anti-frosting (Liu and Li 2012). Among the various inventions inspired by biomimicry, the banana leaf has become a research area of particular interest because of the great potential of the self-cleaning mechanism of its surface (Yuan *et al.* 2013).

A well-known effect of biomimicry is the 'lotus leaf effect', in which the leaf surface is impermeable to dew and raindrops. Water droplets can roll off easily and remove dirt and debris from the surface in the process, which cleans the leaf surface (Adithyavairavan and Subbiah 2011). Nevertheless, surfaces with high contact angles do not always exhibit an excellent water resistance behavior. For instance, red rose petals, which are rich in nanostructures and nano-folds exhibit a water-repellent feature, with strong adhesive forces, despite the presence of wax crystals. The adhesion of rose petals appears greater compared with that of lotus leaves, and this phenomenon is called the

'petal effect' (Wang *et al.* 2014a). Rice leaves demonstrate an excellent superhydrophobicity and special anisotropic sliding properties, whereby water droplets tend to roll along the veins at a slight sliding angle. Because of these characteristics, artificial rice leaves have become important in fluidic direction control, no-loss liquid transportation, and self-cleaning materials (Yao *et al.* 2012).

It is well known that there are typically two states in which a water droplet can occupy on a rough surface (He *et al.* 2004) . The water droplet either sits on the peaks of the rough surface (heterogeneous) or wetting the grooves (homogeneous), depending on how it is formed. The water droplet that sits on the peaks has 'air pockets' along its contact with the surface and hydrophobicity is determined by the water contact angle (Ramlan *et al.* 2018).

Figure 1 shows the Cassie-Baxter schematic illustration for a composite interface with the creation of air pockets, and Fig. 2 shows the relationship between the contact angle and proportion of air trapped within the surface. According to Cassie and Baxter (1944), a water dewdrop exhibits a water contact angle once it is in contact with a rough surface. The presence of air bubbles trapped within a rough surface creates a water contact angle with the solid surface and an air/water interfacial contact angle (Webb *et al.* 2014). Interfacial tension is defined as the presence of an interface between the air and liquid in relation to the surface tension γ_{LV}. When a water dewdrop lies on a solid, the solid-liquid and solid-vapor would develop the interfacial tensions γ_{SL} and γ_{SV}, respectively (Myshkin *et al.* 2005), and described in Eq. 1 below.

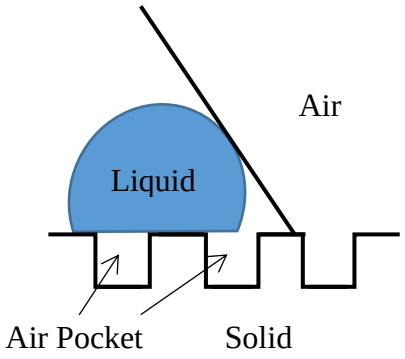

Fig. 1. Cassie-Baxter diagram for a composite interface with air-pockets (new drawing inspired by Ghazali *et al.* (2016))

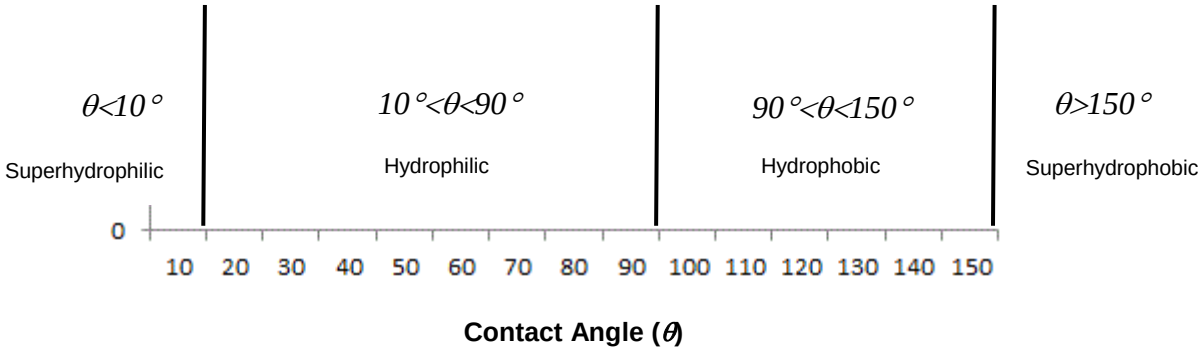

Fig. 2. Relationship of the material wettability and proportion of air trapped within the surface features (new drawing inspired by Liu and Li (2012))

At equilibrium, the three interfacial forces are related to the contact angle as shown by Eq. 1:

$$\gamma_{SV} = \gamma_{SL} + \gamma_{LV} \cdot \cos\theta \quad (1)$$

In studying superhydrophobic surfaces, it is predicted that there would be no adsorption at the interfaces where the surface tension is similar to the surface free energy (Yan *et al.* 2011). The wet area should demonstrate a higher surface energy than the dry area, while the shape of the surface droplet should become more spherical to minimize the energy of the droplet. The film on the surface of the leaf is mainly composed of C and H elements, which constitute an organic wax with a low surface energy. Water droplets on these surfaces lay on the peak of the nanostructures because air bubbles fill the valleys between the papillae under the droplet (Wang *et al.* 2014b).

Moreover, wax crystals are known to be able to reduce the attachment of any environmental impurity caused by cuticular folds with different spacings and shapes (Prüm *et al.* 2013). Several hypotheses have been proposed to explain the mechanisms of attachment reduction on plant surfaces. Roughness, contamination, chemistry, fluid absorption, and wax dissolution are among the proposed mechanisms. In a previous study, the 'banana leaf effect' (BLE) was reported, whereby banana leaves, being used as the water-repellent surface, demonstrated a self-cleaning ability. The BLE was the result of the interaction of the surface micro-features, which consisted of stomata interacting with the external stimuli, such as the load and temperature. The stomata structures on the banana leaves became elongated, thereby closing their apertures towards the sliding action when subjected to hot iron plates (Yuan *et al.* 2013). At the highest temperature of 230 °C under a 16-N load, the stomata showed the largest opening compared with the other samples. In addition to the stomata, the other micro-features responsible for the BLE were the air pockets.

The cleaning mechanism, as reported in an earlier paper (Ghazali *et al.* 2016), is a combined function of the microstructures on the banana leaves consisting of stomata and air pockets. Increasing load and temperature will result in change in dimensions of the stomata, thus initiating inter-diffusion and strengthening the contact between the soil and

leaf surfaces. This result in stronger adhesion between asperities-leaf contact, causing the weaker material to be sloughed off from its original location.

Air pockets provide an interface between the solid, liquid, and air, which influence the contact angle of the solid-liquid-vapor surface and reduce the surface tension. There is a strong relationship between adhesion force and roughness, wherein higher roughness will decrease the adhesion force. The relationship between adhesion strength and roughness were also reported by Sogutlu *et al.* (2016) and Sogutlu (2017), who reported a strong relationship of varnish and glue adhesion strength and surface roughness in their study of surface roughness of wooden bonding surfaces.

There are more than 18 to 35 species of banana plant (Genus: *Musa*) that are suitable for cultivation in an equatorial climate having not more than 3 months of dry season annually (Tock *et al.* 2010). Bananas are endemic to tropical countries in Latin America, the Caribbean, and some of the Asian countries (Philippines, Thailand, India, Indonesia, and Malaysia), which are the main exporters for the fruits. Banana leaves are composed of lignin (16.5%), hemicelluloses (22.4%), cellulose (39.2%), ash (5.2%), wax (4.1%), and resin and soluble materials (12.6%) (Nada and Mohamed 2010).

Banana leaves in Malaysia have been traditionally utilized by the local population for myriad purposes, particularly in food preparation and household chores. Banana leaves as a dressing is also used for skin grafting in order to get a non-adherent and pain-free dressing (Gore and Akolekar 2003). One interesting use is as a cleaning device combined with lubricating action for smooth and effortless ironing, rather like synthetic non-wrinkle preparations available in the market.

In this study, the effects of heat and load on the surface adhesion force, roughness, and contact angle of the banana leaf interface were investigated and correlated with the surface morphology.

EXPERIMENTAL

Material and Methods

Starting materials

Lemak manis (*Musa acuminata* Colla) was cultivated in Agriculture University Park (Serdang, Malaysia) to obtain a controlled growth with a consistent age and breed-type. All of the leaves were sectioned to the dimensions 20 cm × 20 cm prior to the sliding test. Three samples were prepared for each test. All measurements were calculated using simple statistical formulas to derive the average and standard deviation.

Sliding test

A hot iron plate was slid on banana leaves at different loads and temperatures (Table 1) with a fixed speed of 0.006 m/s. These sliding conditions were selected from the actual action of daily ironing works (Azura 2014) with longitudinal sliding directions on both sides. Each sample was kept constant with the applied loads for 20 s and a sliding distance of approximately 0.15 m. The choice of temperature was based on the range used for conventional temperature of iron usage - which is pegged at 200 to 250°C with a temperature lower and two temperatures higher than the pegged value. Data was obtained using simple statistical method to derive the average value and standard deviation.

Table 1. Sample Labels for the Sliding Test on the Surface of the Banana Leaf at Different Temperatures and Loads

Load (N)	Temperature (°C)			
	100	200	300	500
5	a	b	e	f
10	c	d	g	h
15	i	j	m	n
30	k	l	o	p

Microstructure and surface examination

The samples (banana leaves) were rinsed in 0.1 M sodium cacodylate buffer, dehydrated at room temperature in a graded series of ethanol, and subsequently dried in hexamethyldisilazane (Hazrin-Chong and Manefield 2012) prior to morphological observations with scanning electron microscopy (SEM) (LEO 1450VP, ZEISS, United Kingdom). The dried samples were mounted on stubs and stored in air exposed to dry silica gel for 12 h before being gold coated.

Roughness and adhesion force

The roughness and adhesion force of the treated banana leaves were determined using an atomic force microscope (AFM) (Park System XE-Series, KOREA) with a cantilever contact (PPP-CONTSCR 10M, Park System XE-Series, KOREA). AFM is used to characterized the roughness and surface roughness has been regarded as one of the most important surface properties (Mohammad *et al.* 2011). The test was carried out in BioNano Technology R&D Centre (BINATAM), Fatih University, Turkey. The average temperature in the laboratory was 10±2°C, and relative humidity was 66±5%.

The roughness was evaluated using the adhesion force and number of bumps. Furthermore, the adhesion force was determined from the pull-off force measured by the force-distance curve (Meine *et al.* 2004). The measurements were repeated at four different locations for five times. Roughness was determined using Eq. 2.

$$R_a = \frac{1}{L} \int_0^L |Z(x)| dx \quad (2)$$

As described in ASME B46.1, R_a is the arithmetic average of the absolute values of the profile height deviations from the mean line, recorded within the evaluation length. Simply put, R_a is the average of a set of individual measurements of a surfaces peaks and valleys. L is evaluation length and $Z(x)$ is the profile height function.

Adhesion force, F is calculated based on Eq. 3. The parameter k is the spring constant of the cantilever, and x is the cantilever deflection.

$$F = kx \quad (3)$$

Roughness was evaluated using the non-contact mode, whereas adhesion force used the contact mode, since the banana surface is rough. A scan size of 20 μm × 20 μm was used to obtain a sufficient amount of bumps for surface characterization and to maintain sufficient resolution for accurate measurement.

Contact angle measurement

The wettability was determined by evaluating the contact angle. All of the samples were arranged horizontally on the glass slides. The standard water contact angle

was determined based on ASTM D7334-08 (2013) with a 10-s duration to ensure droplet stability. This was repeated at five different locations for reproducible values. Calculation for the contact angle is done using Eq. 4,

$$\cos\theta = \frac{(\gamma_{SV} - \gamma_{SL})}{\gamma_{LV}} \quad (4)$$

where θ is the contact angle, γ_{SV} is the solid-vapor surface tension, γ_{SL} is the solid-liquid surface tension and γ_{LV} is the liquid-vapor surface tension.

RESULTS AND DISCUSSION

Microstructure and Surface Examination

Figure 3 shows a typical microstructure of a fresh banana leaf surface with distinct features, such as stomata, valleys, and air pockets. The opening of the stomata of approximately 20 μm with a narrow distance between the valleys created air pockets. The air pockets were created by the air trapped in the cavities of the rough surface that resulted in a composite solid-air-liquid interface (Bhushan and Jung 2007). The banana leaf surface was found to be comprised of papillose epidermal cells, which are responsible for the creation of papillae in forming peaks and valleys to create a nanostructure with air pockets on the entire surface (Bhushan and Jung 2011).

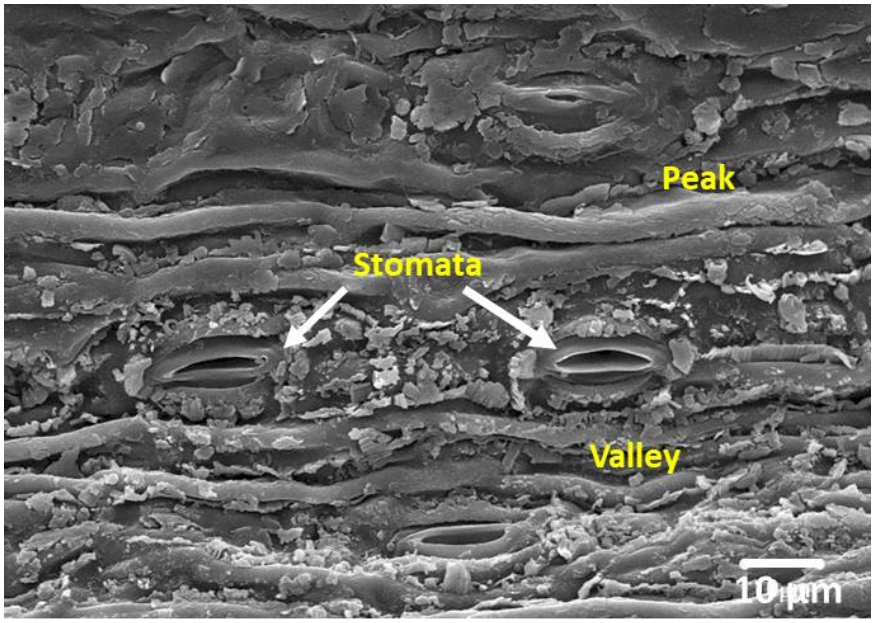

Fig. 3. SEM image of the banana leaf surface prior to the load and temperature tests

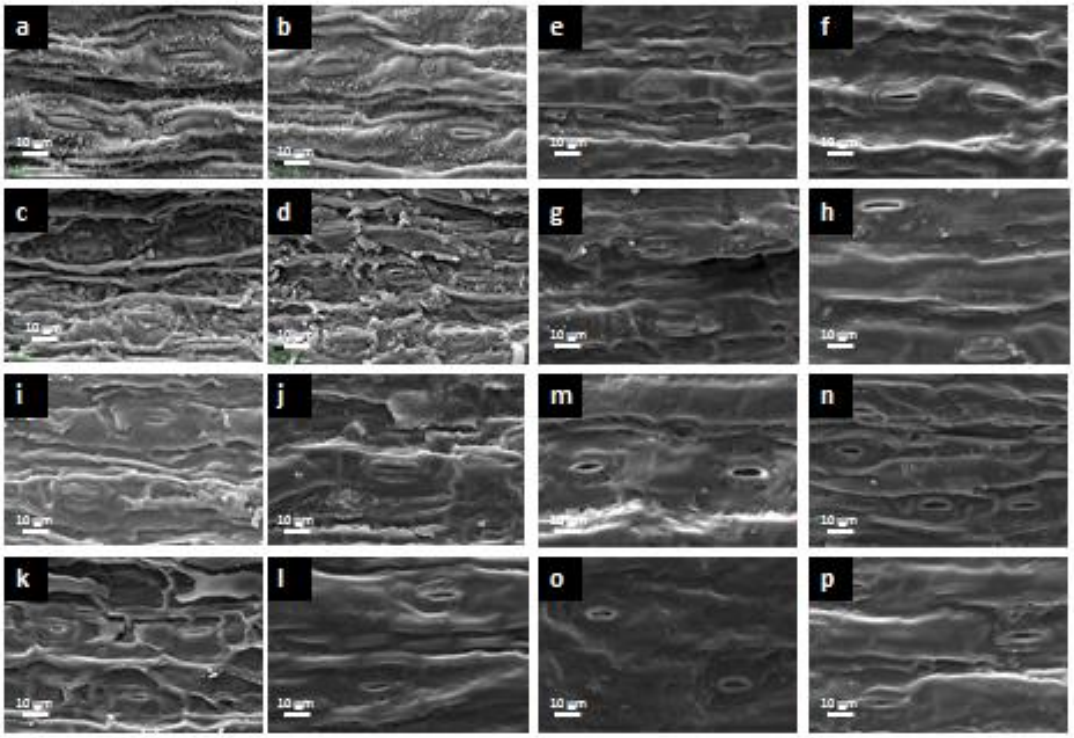

Fig. 4. SEM images of the banana leaf surface under different loads and temperatures: (a) 5 N and 100 °C, (b) 5 N and 200 °C, (c) 10 N and 100 °C, (d) 10 N and 200 °C, (e) 5 N and 300 °C, (f) 5 N and 500 °C, (g) 10 N and 300 °C, (h) 10 N and 500 °C, (i) 15 N and 100 °C, (j) 15 N and 200 °C, (k) 30 N and 100 °C, (l) 30 N and 200 °C, (m) 15 N and 300 °C, (n) 15 N and 500 °C, (o) 30 N and 300 °C, and (p) 30 N and 500 °C

The SEM images in Fig. 4 show the BLE map. The leaf surfaces in Figs. 4a to 4d showed similar morphologies. Under the conditions of 100 °C to 200 °C and 5 N to 10 N, the stomata were generally closed, and ridges ran parallel in the direction of the sliding force. The distance between the ridges was approximately 6 μm to 8 μm. A copious amount of wax was present on the surface, which formed ridges. The next block of morphologies is shown in Figs. 4e to 4h. This block corresponded to both the increase in the temperature (300 °C to 500 °C) and load (5 N to 10 N). The stomata were closed, the distance between ridges was wider (approximately 10 μm to 12 μm), and deposited wax disappeared.

Figure 4i shows that as the load increased (15 N), the block exhibited narrower ridges and a decreased wax deposition, despite it having a similar morphology as the first block (Figs. 4a to 4d). Figures 4e, 4g, and 4j show similar features, but Fig. 4j reveals wider ridges with flattened wax deposits and closed stomata. At a higher temperature (300 °C), a decrease in the stomata size and increase in the width of the ridges were observed (Figs. 4e, 4g, 4m, and 4o). These outcomes were caused by the flattening of the waxes, which covered the stomata diameter and thereby decreased the size. The same explanation could be applied to Figs. 4f, 4h, 4n, and 4p, but with a smaller stomata size. This effect was observed as the load increased, which resulted in wider ridges and a smaller wax deposit. Overall, increases in the sliding force and temperature flattened the wax deposits and covered the stomata opening.

The BLE map showed transitions in the morphological features with a change in the imposed conditions, *i.e.*, the temperature and sliding force. The first morphological

transition occurred at a load of 10 N, followed by another transition at 15 N and a complete change at 30 N. The transition in the morphological features because of the temperature occurred at 300 °C, which persisted up to 500 °C.

The stomata structures exhibited remarkable changes because of the temperature and load. The presence of air pockets increased the ability of the surface to trap air, which allowed the water droplets to rest on the peak of wax asperities on the surface. The particles in the spaces of the ridges could adhere to the water droplets through adhesion. The water droplets appeared to have the ability to lift particles that resided in the spaces in the ridges, which removed impurities from the surface. This observation was first reported at room temperature by Ghazali *et al.* (2016).

For fresh leaves in general, the opening and closure of the stomata are affected by humidity, water, and carbon dioxide. The inflation (in) and deflation (out) of water from the stomata with the load and heat applied altered the stomata size (Shepherd and Griffiths 2006). Nevertheless, heat was not applied from a direct source, but from the outdoor temperature (above 35 °C) (Schreiber 2001). Even at such low temperatures, morphological changes were reported by Hassan *et al.* (2017) at room temperature and by Ghazali *et al.* (2016).

Roughness and adhesion force

The fresh leaf roughness of 0.25 μm increased up to 1.12 μm, after various temperatures and loads were applied and as the wax was removed. The surface roughness for a load of 30 N increased from 0.79 μm ± 0.21 μm at 100 °C to 1.12 μm ± 0.30 μm at 500 °C. In general, a decrease in the adhesion force with an increasing roughness was observed, which is shown in Figs. 5 and 6. For the self-cleaning mechanism of most biological surfaces, there is an association between the surface roughness, reduction in particle adhesion, and water repellency (Myshkin *et al.* 2005). The same phenomena, including all of the mechanisms, were also observed in this study. Table 2 exhibited the roughness measured on the surface of banana leaf at different temperatures and loads.

Table 2. Roughness measured by AFM on the Surface of the Banana Leaf at Different Temperatures and Loads

Load (N)	Temperature (°C)			
	100	200	300	500
	R_a (μm)			
5	0.271±0.002	0.794±0.213	0.728±0.334	0.821±0.004
10	0.586±0.02	0.481±0.029	0.521±0.096	0.236±0.028
15	0.152±0.003	0.584±0.021	0.675±0.245	1.113±0.35
30	0.341±0.081	0.62±0.07	0.902±0.14	1.119±0.297

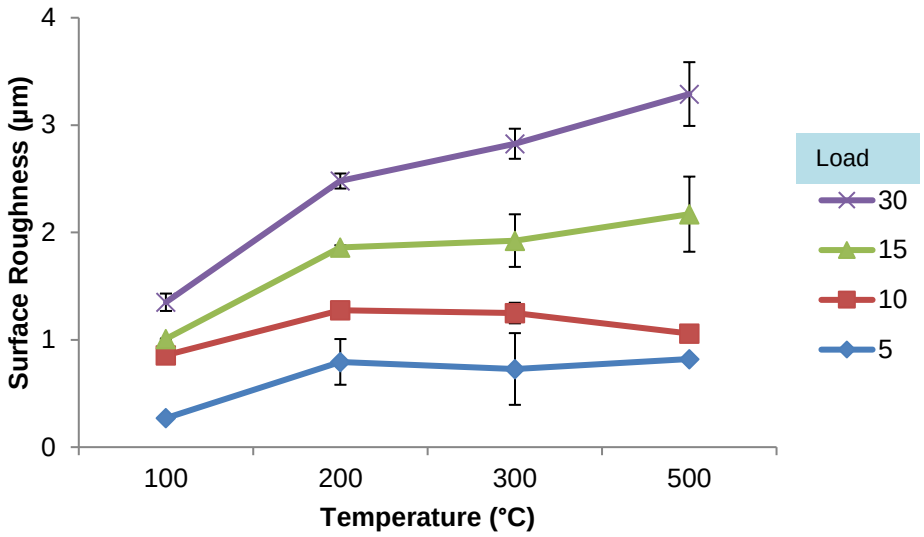

Fig. 5. Measured roughness of the different applied loads at different temperatures

The adhesive force of the fresh leaf deformed elastically because of the moisture on the surface, which exposed a large real contact area between the tip of the AFM probe and leaf, and thus increased the adhesive force (Yuan *et al.* 2013). In contrast, the dried leaf with less moisture demonstrated a decreased adhesive force because of the similarly smaller real contact area (Burton and Bhushan 2006). Figure 6 show that there was a reduction in the adhesion force because of the loss of moisture as the sliding temperature increased up to 500 °C. The adhesion force decreased from 6.39 nN ± 0.42 nN at 100 °C to 0.50 nN ± 0.50 nN at 500 °C with a load of 30 N, which was because of the loss of moisture as the wax reached its melting point at 82.9 °C (Hassan *et al.* 2017).

When the asperities of two sliding surfaces are in contact, another source of frictional force is attributed to the elastic, plastic, or viscoelastic deformation, depending on the material behavior (Myshkin *et al.* 2005). There could be equal and opposite forces, which would result in neutralized forces, or imbalanced forces from one surface having stronger forces than the other. A comparison between fresh (Fig. 3) and soiled banana leaf surfaces (Fig. 4) showed that the fresh unsoiled surfaces could attract particles/materials from the soiled surface. This was the origin of the ability of the surface to self-clean. Adhesion force that measured on the surface of the banana leaf at different temperatures and loads showed are listed in Table 3.

Table 3. Adhesion force measured by AFM on the Surface of the Banana Leaf at Different Temperatures and Loads

Load (N)	Temperature (°C)			
	100	200	300	500
	nN			
5	6.392±0.424	2.769±1.66	0.899±0.182	1.308±0.91
10	4.094±1.37	0.964±0.211	1.152±0.114	1.37±0.32
15	7.14±3.19	0.764±0.686	1.424±1.11	0.313±0.058
30	3.334±0.71	0.825±0.588	0.653±0.91	0.499±0.495

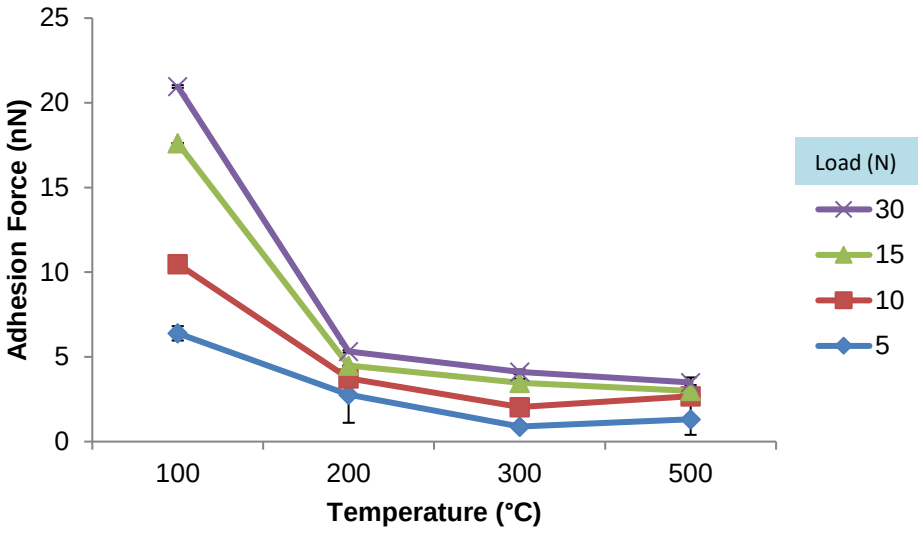

Fig. 6. Measured adhesion forces of the different applied loads at different temperatures

It was reported in a separate study that the effect of self-cleaning is the result of the twin effects of the surface roughness and hydrophobicity (Shirtcliffe *et al.* 2010). A higher surface roughness contributed to a higher contact angle, and hence a higher hydrophobicity (Jemat *et al.* 2013). The combined effect allowed the droplets to stay on the top of the surface and roll off together with the soil.

Theoretically, a high roughness and low adhesion force can lead to a greater contact angle (Burton and Bhushan 2006). Nonetheless, in the present study, the application of heat and load affected the leaf structure, which resulted in a lower contact angle at a higher load and temperature. At a lower temperature, the adhesion force was higher and a suction effect attracted asperities from the dirty surface. When the hot plate came into contact with the banana leaf surface, the surface energy of the banana leaf decreased as the wax melted and compacted.

Contact angle

Figure 7 illustrates the contact angle measurement data obtained from the experiments using Eq. 4. The contact angles remarkably decreased as the wax was removed from the surface, as is shown in Fig. 4. A combination of wax and bumps was the main contributor to the behavior of the contact angles (Burton and Bhushan 2006). The closed stomata and wider ridges increased the surface contact area and thus reduced the contact angle measurement. Tabulated data on the contact angle is showed in Table 4.

Table 4. Measured contact angle on the Surface of the Banana Leaf at Different Temperatures and Loads

Load (N)	Temperature (°C)			
	100	200	300	500
	°			
5	120.68±6.32	111.26±2.62	113.42±2.74	105.75±3.07
10	117.64±4.63	111.86±3.25	112.08±2.08	106.4±4.5
15	122.92±6.91	120.56±2.66	114.46±3.85	97.02±3.2
30	124.82±6.03	120.44±2.46	110.6±2.67	104.02±3.9

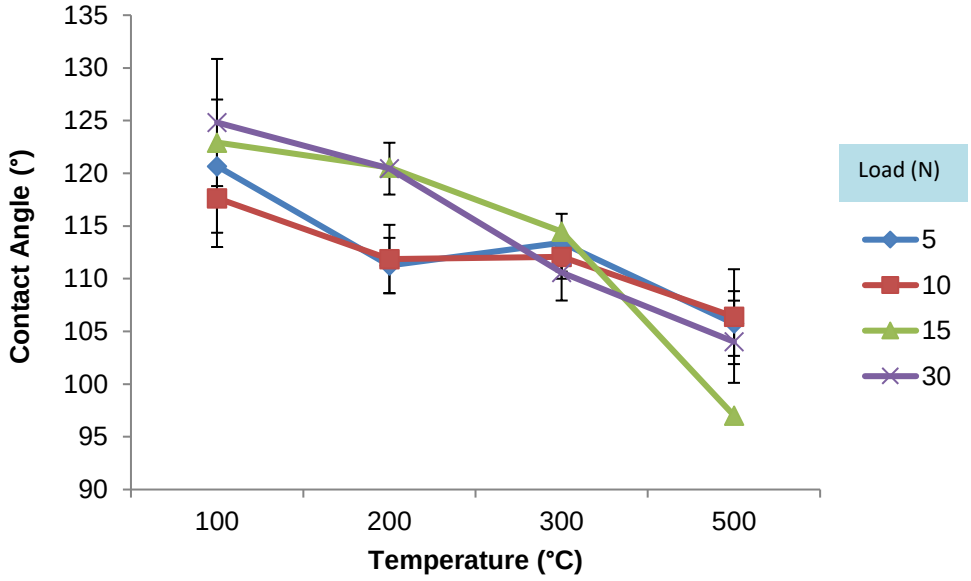

Fig. 7. Graph showing the measured static contact angles of the different applied loads at different temperatures

The initial experiment performed on the fresh leaf showed that the contact angle was approximately 130°. The contact angle reported from the extracted wax was 133° (Hassan *et al.* 2017), which verified that the existing wax on the surface contributed to the contact angle. Nevertheless, there were no major changes in the contact angle between the fresh and treated leaves, despite a decreasing contact angle with increasing loads and temperatures, because the value remained in the hydrophobic state with a contact angle above 90°. This showed that loads and temperatures of up to 30 N and 500 °C, respectively, had an unremarkable effect on the wettability.

Furthermore, the comparison of the surface morphology and contact angle at 100 °C, 200 °C, 300 °C, and 500 °C for a load of 30 N is demonstrated in Fig. 8. The surface morphology consisted of stomata, ridges running parallel in the direction of sliding, and molten wax. Based on the micrographs at 200 °C and 500 °C, the features were similar with apparent ridges, in contrast to the features present at 100 °C and 300 °C. The stomata sizes at 100 °C and 300 °C were smaller than at 200 °C and 500 °C, as was described earlier. Therefore, it was established that smaller-sized stomata resulted in higher contact angles at 100 °C and 300 °C compared with the contact angles at 200 °C and 500 °C.

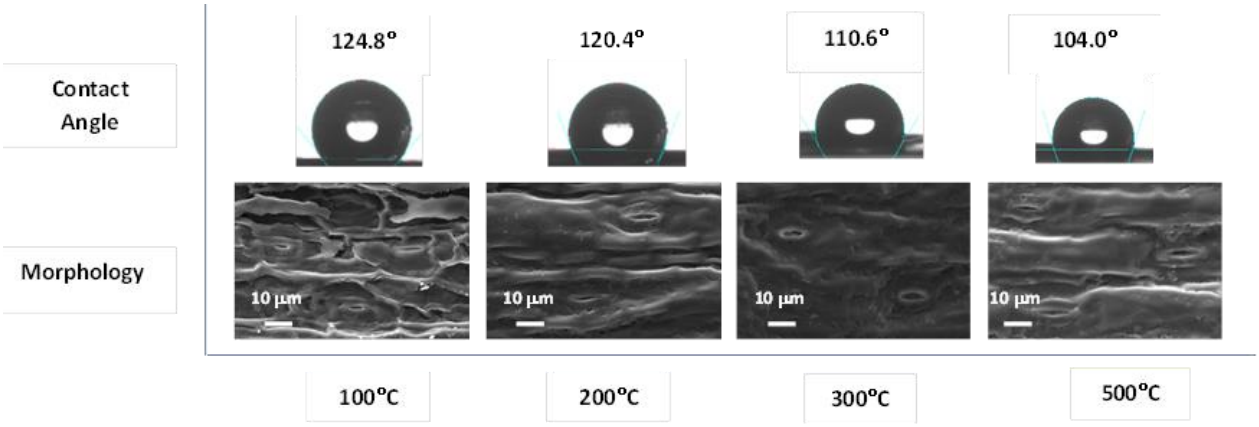

Fig. 8. Surface morphology and contact angles at 100 °C, 200 °C, 300 °C, and 500 °C for a load of 30 N

CONCLUSIONS

1. The morphological feature changes of *Musa acuminate* Colla leaves were evaluated using scanning electron microscopy (SEM). The first morphological transition occurred when a load of 5 N to 10 N was applied at 100 °C and 200 °C; stomata were closed and the ridges ran parallel in the direction of the sliding force. The changes of features were followed by another transition at higher temperature (300 °C and 500 °C), at which point the stomata were closed, the distances became wider between ridges, and the wax deposits disappeared. The transition in the morphological features secondary to the temperature occurred at 300 °C and persisted to 500 °C.
2. Generally, as the load increased (15 N to 30 N), wax deposition keep decreasing and flattened with wider ridges and closed stomata. Increases in the sliding force and temperature flattened the wax deposits and covered the stomata openings.
3. Changes in both the temperature and load also affected the roughness, adhesion force, and contact angle. At higher loads (15 N and 30 N) and temperatures (300 °C and 500 °C), the lowest adhesion force was observed. In relation to the loads 15 N and 30 N at temperatures of 300 °C and 500 °C, the contact angle was 97° and 104°, and the surface roughness was 1.11 µm and 1.12 µm, respectively.
4. The cleansing effect was postulated to be a result of the interaction between the water droplets, wax deposits, and asperities, which ultimately led to the removal of particles in the air pockets *via* adhesion. Increasing load and temperature changed the stomata dimensions, resulting in weaker adhesion between asperities and surface contacts and sloughing off the asperities together with the water droplets.

ACKNOWLEDGEMENTS

This work was financially supported by the grant FRGS/2/2013/TK04/UKM/02/2, and the authors are thankful to CRIM UKM, the Faculty of Bioengineering UM, and Dr. Armin Rajabi from UKM and BINATAM (Fatih University, Istanbul, Turkey) for the support.

REFERENCES CITED

Adithyavairavan, M., and Subbiah, S. (2011). "A morphological study on direct polymer cast micro-textured hydrophobic surfaces," *Surf. Coat. Tech.* 205(20), 4764-4770. DOI: 10.1016/j.surfcoat.2011.03.082

ASTM D7334-08 (2013). "Standard practice for surface wettability of coatings, substrates and pigments by advancing contact angle measurement," ASTM International, West Conshohocken, PA.

Azura, F. (2014). *Keberkesanan Daun Pisang sebagai Pelincir dan Pembersih Seterika* [*Effectiveness of Banana Leaves as Lubricants and Iron Cleaners*], Master's Thesis, Universiti Kebangsaan, Bangi, Malaysia.

Bhushan, B., and Jung, Y. C. (2007). "Wetting study of patterned surfaces for superhydrophobicity," *Ultramicroscopy* 107(10-11), 1033–1041. DOI: 10.1016/j.ultramic.2007.05.002

Bhushan, B., and Jung, Y. C. (2011). "Natural and biomimetic artificial surfaces for superhydrophobicity, self-cleaning, low adhesion, and drag reduction," *Prog. Mater. Sci.* 56 (1), 1–108. DOI: 10.1016/j.pmatsci.2010.04.003

Burton, Z., and Bhushan, B. (2006). "Surface characterization and adhesion and friction properties of hydrophobic leaf surfaces," *Ultramicroscopy* 106(8-9), 709-719. DOI: 10.1016/j.ultramic.2005.10.007

Cassie, A. B. D., and Baxter, S. (1944). "Wettability of porous surfaces," *T. Faraday Soc.* 40, 546-551. DOI: 10.1039/tf9444000546

Ghazali, M. J., Hassan, H. A., Azhari, C. H., and Mamat, F. A. (2016). "The bio-adhesion behaviour of banana leaves as soil remover at elevated temperatures," *Tribology Online* 11(2) 264-271. DOI: 10.2474/trol.11.264

Gore, M. A., and Akolekar, D. (2003). "Banana leaf dressing for skin graft donor areas," 29(5), *Burns* 483-486. DOI: 10.1016/S0305-4179(03)00049-4

Hassan, H. A., Ghazali, M. J., Zainuddin, N. M., and Azhari, C. H. (2017). "Kesan lilin ke atas sifat hidrofobik permukaan daun pisang (Wax effect on hydrophobic properties of banana leaves)," *Jurnal Kejuruteraan* 29(1), 1-7.

Hazrin-Chong, N. H., and Manefield, M. (2012). "An alternative SEM drying method using hexamethyldisilazane (HMDS) for microbial cell attachment studies on sub-bituminous coal," *J. Microbiol. Meth.* 90(2), 96-99. DOI: 10.1016/j.mimet.2012.04.014

He, B., Lee, J., and Patankar, N. A. (2004). "Contact angle hysteresis on rough hydrophobic surfaces," *Colloids and Surfaces A: Physicochemical and Engineering Aspects*, 248(April), 101–104. DOI: 10.1016/j.colsurfa.2004.09.006

Jemat, A., Ghazali, M. J., Razali, M., and Otsuka, Y. (2013). "Microstructural, surface roughness and wettability of titanium alloy coated by yzp-30wt% TiO_2 for dental application," *Jurnal Teknologi*, 80(2), 45–50. DOI: 10.11113/jt.v80.10875

Mohammad, A. W., Hilal, N., Lim, Y. P., Mohd Amin, I. N. H., and Raslan, R. (2011). "Atomic force microscopy as a tool for asymmetric polymeric membrane characterization," *Sains Malaysiana* 40(3), 237–244.

Nada, A. M. A., and Mohamed, S. H. (2010). "Banana leaves as adsorbents for removal of metal ions from waste water," *Carbohydrate Polymers*, 82(4), 1025–1030. DOI: 10.1016/j.carbpol.2010.03.004

Prüm, B., Florian Bohn, H., Seidel, R., Rubach, S., and Speck, T. (2013). "Plant surfaces with cuticular folds and their replicas: Influence of microstructuring and surface

chemistry on the attachment of a leaf beetle," *Acta Biomaterialia*, 9(5), 6360–6368. DOI: 10.1016/j.actbio.2013.01.030

Ramlan, N., Mohd Zamri, N. W., Maskat, M. Y., Md Jamil, M. S., Chin, O. H., Lau, Y. T., and Zubairi, S. I. (2018). "Effect of plasma treatment (He / CH_4) on glass surface for the reduction of powder flux adhesion in the spray drying process," *Sains Malaysiana* 47(6), 1147–1155. DOI: 10.17576/jsm-2018-4706-10

Tock, J. Y., Lai, C. L., Lee, K. T., Tan, K. T., and Bhatia, S. (2010). "Banana biomass as potential renewable energy resource : A Malaysian case study," *Renewable and Sustainable Energy Reviews*, 14, 798–805. DOI: 10.1016/j.rser.2009.10.010

Wang, G., Guo, Z., and Liu, W. (2014a). "Interfacial effects of superhydrophobic plant surfaces: A review," *J. Bionic Eng.* 11(3), 325-345. DOI: 10.1016/S1672-6529(14)60047-0

Wang, T., Chang, L., Hatton, B., Kong, J., Chen, G., Jia, Y., Xiong, D., and Wong, C. (2014b). "Preparation and hydrophobicity of biomorphic ZnO/carbon based on a lotus-leaf template," *Materials Science and Engineering: C* 43, 310-316. DOI: 10.1016/j.msec.2014.07.022

Webb, H. K., Crawford, R. J., and Ivanova, E. P. (2014). "Wettability of natural superhydrophobic surfaces," *Adv. Colloid Interfac.* 210, 58-64. DOI: 10.1016/j.cis.2014.01.020

Yan, Y. Y., Gao, N., and Barthlott, W. (2011). "Mimicking natural superhydrophobic surfaces and grasping the wetting process: A review on recent progress in preparing superhydrophobic surfaces," *Adv. Colloid Interfac.* 169(2) 80-105. DOI: 10.1016/j.cis.2011.08.005

Yao, J., Wang, J., Yu, Y., Yang, H., and Xu, Y. (2012). "Biomimetic fabrication and characterization of an artificial rice leaf surface with anisotropic wetting," *Chinese Sci. Bull.* 57(20), 2631-2634. DOI: 10.1007/s11434-012-5220-1

Yuan, Z., Wang, X., Bin, J., Peng, C., Xing, S., Wang, M., Xiao, J., Zeng, J., Xie, Y., Xiao, X., *et al*. (2013). "A novel fabrication of a superhydrophobic surface with highly similar hierarchical structure of the lotus leaf on a copper sheet," *Appl. Surf. Sci.* 285(Part B), 205-210. DOI: 10.1016/j.apsusc.2013.08.037

Article submitted: January 16, 2019; Peer review completed: March 17, 2019; Revised version received: April 3, 2019; Accepted: May 19, 2019; Published: September 3, 2019.
DOI: 10.15376/biores.14.4.8331-8344